



A calcium signalling network activates vacuolar K⁺ remobilization to enable plant adaptation to low-K environments

Ren-Jie Tang¹, Fu-Geng Zhao^{2,3}, Yang Yang², Chao Wang¹, Kunlun Li¹, Thomas J. Kleist¹, Peggy G. Lemaux ¹ and Sheng Luan ¹

Potassium (K) is an essential nutrient, but levels of the free K ions (K⁺) in soil are often limiting, imposing a constant stress on plants. We have discovered a calcium (Ca²⁺)-dependent signalling network, consisting of two calcineurin B-like (CBL) Ca²⁺ sensors and a quartet of CBL-interacting protein kinases (CIPKs), which plays a key role in plant response to K⁺ starvation. The mutant plants lacking two CBLs (CBL2 and CBL3) were severely stunted under low-K conditions. Interestingly, the *cbl2 cbl3* mutant was normal in K⁺ uptake but impaired in K⁺ remobilization from vacuoles. Four CIPKs—CIPK3, 9, 23 and 26—were identified as partners of CBL2 and CBL3 that together regulate K⁺ homeostasis through activating vacuolar K⁺ efflux to the cytoplasm. The vacuolar two-pore K⁺ (TPK) channels were directly activated by the vacuolar CBL-CIPK modules in a Ca²⁺-dependent manner, presenting a mechanism for the activation of vacuolar K⁺ remobilization that plays an important role in plant adaptation to K⁺ deficiency.

otassium (K) is an essential macronutrient for plant growth and development. In contrast to a relatively high and stable K+ concentration (around 100 mM) in the cytoplasm, bio-available K⁺ levels in most natural soils are limited, typically in the submillimolar range^{1,2}. To cope with the low-K conditions, plant roots are equipped with an array of transporters and channels capable of pulling K⁺ into the cell against the electrochemical gradient^{3,4}. In particular, a K+ channel (AKT1) and a K+/H+ symporter (HAK5) are two major facilitators for root K+ acquisition when external K+ concentration falls below 0.2 mM (refs. 5,6). Disruption of AKT1 and HAK5 leads to considerable loss of K+ uptake capacity in Arabidopsis roots, coupled with severe plant growth defects under low-K conditions^{5,7}. Both AKT1 and HAK5 are activated by calcineurin B-like (CBL) calcium (Ca2+) sensors and their interacting protein kinases (CIPKs). In plants, CBLs and CIPKs generally form membrane-anchored CBL-CIPK complexes that serve as molecular modules in decoding Ca²⁺ signals⁸. It has become increasingly evident that the CBL-CIPK signalling network plays a primary role in the regulation of membrane transport processes in plant cells^{8,9}. In the case of K⁺ uptake, CBL1 and CBL9 physically interact with their downstream kinase CIPK23 to recruit the CBL1/9-CIPK complexes to the plasma membrane, where they activate the AKT1 and HAK5 through phosphorylation¹⁰⁻¹². This CBL-CIPK-mediated signalling pathway, conserved in different plant species, is essential for plants to survive low-K environments¹²⁻¹⁴.

After uptake from the soil, K^+ moves into the stele to be distributed throughout the plant via vasculature^{15,16}. Once arriving at the 'sink' cells (for example, mesophyll cells in the leaf), K^+ is used in cellular metabolism and osmoregulation with excess K^+ sequestered into the vacuoles by tonoplast K^+/H^+ antiporters^{17,18}. In addition to supporting turgor pressure for cell expansion and movement, the vacuolar K^+ pool can also be remobilized into the cytoplasm in response to K^+ deficiency.

Two major mechanisms operate in parallel for plants to respond and adapt to K+ deficiency: boosting root K+ uptake and remobilizing local vacuolar K⁺ stores^{4,19,20}. When external K⁺ levels are minimal, retrieving K+ from the vacuolar store may become the only way for plants to survive and grow during K+ starvation. However, the molecular components and signalling pathways that regulate vacuolar K⁺ remobilization remain largely unknown. In this study, we identified a signalling pathway that involves CBL-CIPK modules in the regulation of vacuolar K+ remobilization. Together with the previously described plasma membrane CBL-CIPK pathway, our finding of the tonoplast CBL-CIPK pathway highlights a central function for the CBL-CIPK signalling network in plant low-K response through orchestrating the activities of multiple K+ transporters for K+ uptake from the soil and remobilization from the vacuolar store. Because mutants lacking the vacuolar CBL-CIPK pathway display more severe growth defects under low-K conditions compared with those devoid of the plasma membrane CBL-CIPK pathway, we conclude that vacuolar K⁺ remobilization functions as a primary mechanism for plants to respond and adapt to low-K environments.

Results

The *cbl2 cbl3* double mutant is hypersensitive to low-K conditions. To identify molecular components that may contribute to vacuolar K⁺ remobilization, we designed a germination-based strategy to screen for mutants that require an external K⁺ supply to support early seedling establishment. This approach specifically targets active K⁺ remobilization from seed storage vacuoles during the seed germination process²¹. Indeed, wild-type *Arabidopsis* seeds germinated well and established normal seedlings in distilled water without external supply of mineral nutrients, solely relying on minerals from seed storage vacuoles (Supplementary Fig. 1). In principle, mutations in genes responsible for nutrient retrieval from vacuoles

¹Department of Plant and Microbial Biology, University of California, Berkeley, CA, USA. ²Nanjing University-Nanjing Forestry University Joint Institute for Plant Molecular Biology, State Key Laboratory for Pharmaceutical Biotechnology, College of Life Sciences, Nanjing University, Nanjing, China. ³These authors contributed equally: Ren-Jie Tang, Fu-Geng Zhao. [∞]e-mail: sluan@berkeley.edu

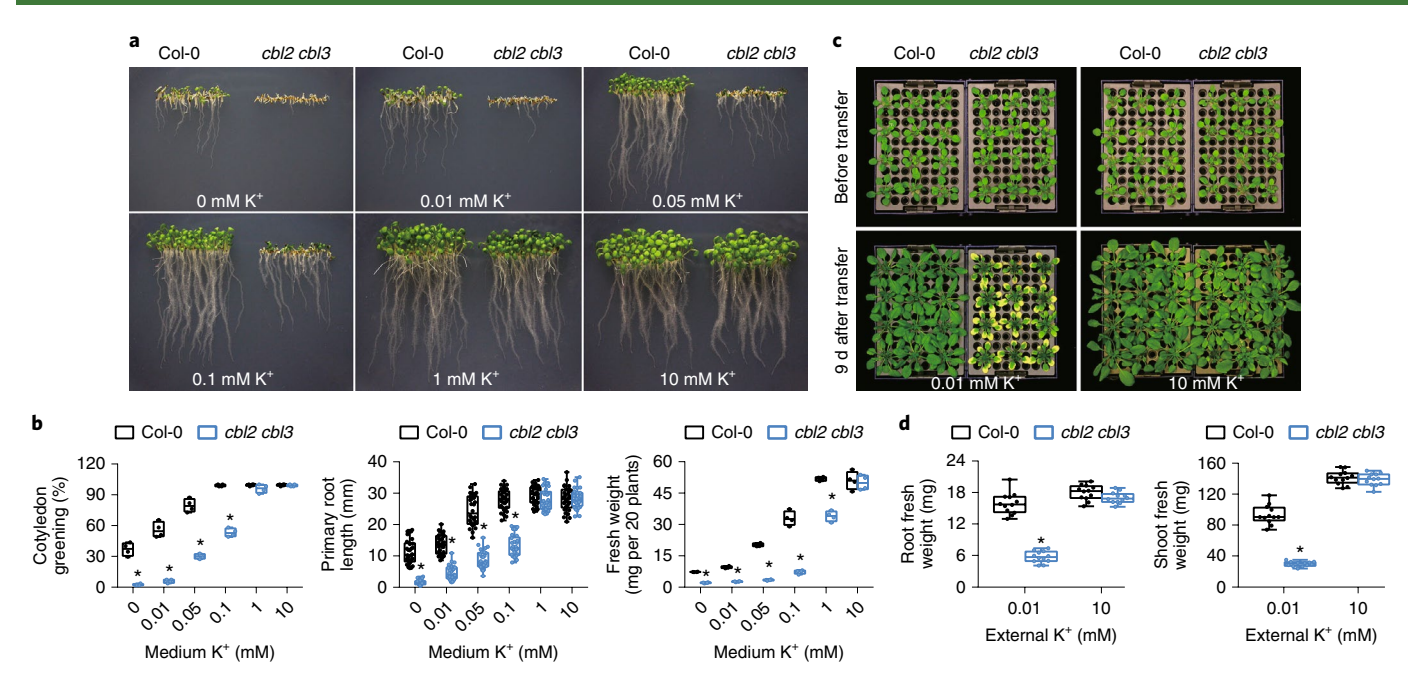


Fig. 1 | How cbl2 cbl3 mutant plants are hypersensitive to external K+ deficiency. a, Seed germination of wild type (Col-0) and cbl2 cbl3 in the presence of different external K+ concentrations. Representative images show eight-day-old seedlings after direct germination on the K-free growth medium supplemented with indicated concentrations of KCI (n=4 biological replicates). **b**, Measurement of cotyledon greening percentage (n=4 biological replicates), primary root length (n=30, independent samples collected from four experiments) and seedling fresh weight (n=4 biological replicates) at the end of the seed germination assay as shown in a. Box plots show the minimum, 25th percentile, median, 75th percentile and maximum of the data points. Asterisks indicate statistically significant differences compared with the wild type by two-tailed Student's t-tests, *P < 0.05. The exact P values are as follows: for cotyledon greening, from left to right, $P = 3.83 \times 10^{-5}$, 1.26×10^{-5} , 6.46×10^{-6} , 5.70×10^{-7} , 0.129, 0.537; for primary root length, from left to right, $P < 1.0 \times 10^{-15}$, $< 1.0 \times 10^{$ 7.22 × 10⁻⁶, 9.78 × 10⁻⁶, 0.739. **c**, Growth phenotype of wild-type and cbl2 cbl3 plants during K⁺-starvation treatment. Wild-type and mutant plants were grown under K-replete conditions (10 mM K⁺) for 16 d and then transferred to new hydroponic solutions containing either sufficient K⁺ (10 mM) or insufficient K⁺ (0.01 mM) for another 9 d. Photographs were taken before the transfer and at the end of the 9-d treatment, respectively. Independent experiments were repeated three times. d, Root and shoot fresh weight of wild-type and cbl2 cbl3 plants on the ninth day after transferring plants to the new hydroponic solutions. Box plots show the minimum, 25th percentile, median, 75th percentile and maximum of the data points. Asterisks indicate statistically significant differences compared with the wild type by two-tailed Student's t-tests, *P < 0.05. Data are from 12 independent biological samples (n=12). The exact P values are as follows: for root fresh weight, at 0.01 and 10, $P=3.37\times10^{-13}$ and 0.0656, respectively; for shoot fresh weight, at 0.01 and 10, $P=3.37\times10^{-13}$ and 0.0656, respectively; for shoot fresh weight, at 0.01 and 10, $P=3.37\times10^{-13}$ and 0.0656, respectively; for shoot fresh weight, at 0.01 and 10, $P=3.37\times10^{-13}$ and 0.0656, respectively; for shoot fresh weight, at 0.01 and 10, $P=3.37\times10^{-13}$ and 0.0656, respectively; for shoot fresh weight, at 0.01 and 10, $P=3.37\times10^{-13}$ and 0.0656, respectively; for shoot fresh weight, at 0.01 and 10, $P=3.37\times10^{-13}$ and 0.0656, respectively; for shoot fresh weight, at 0.01 and 10, $P=3.37\times10^{-13}$ and 0.0656, respectively; for shoot fresh weight, at 0.01 and 10, $P=3.37\times10^{-13}$ and 0.0656, respectively; for shoot fresh weight, at 0.01 and 10, $P=3.37\times10^{-13}$ and 0.0656, respectively; for shoot fresh weight, at 0.01 and 10, $P=3.37\times10^{-13}$ and 0.0656, respectively; for shoot fresh weight, at 0.01 and 10, $P=3.37\times10^{-13}$ and 0.0656, respectively. 10, $P = 2.40 \times 10^{-14}$ and 0.465, respectively.

would result in defects during seed germination. When screening mutants with transfer DNA (T-DNA) insertions in various genes encoding K⁺ transporters and potential regulators, we identified several mutants with a dramatic defect in seedling establishment. One such mutant harbours T-DNA insertions in both *CBL2* and *CBL3* genes (Supplementary Fig. 1), which encode two major CBLs anchored to the tonoplast²². To verify a K⁺-specific effect on the phenotype, we subsequently germinated the seeds under various external K⁺ regimes and found that the addition of 1–10 mM K⁺ into the medium rescued seedling establishment of the *cbl2 cbl3* mutant, whereas 0.01–0.1 mM K⁺ did not (Fig. 1a,b).

Previous work suggests that CBL2 and CBL3 modulate tonoplast V-ATPase activity, which in turn regulates many aspects of plant growth and ion homeostasis²². We thus examined whether vacuolar H⁺-ATPase is involved in low-K response by testing the germination of *vha-a2 a3*, a tonoplast V-ATPase null mutant²³, on the medium containing low levels of K⁺. Unlike the *cbl2 cbl3* mutant, *vha-a2 a3* seeds germinated like the wild type (Supplementary Fig. 2), indicating that CBL2 and CBL3 regulate low-K response in a tonoplast V-ATPase-independent manner.

CBL1 and CBL9, which are targeted to the plasma membrane, function as essential Ca²⁺ sensors required for activation of root K⁺ uptake during K⁺ deficiency^{10,11,24}. However, under the experimental conditions designed for screening the K⁺-remobilization defect,

cbl1 cbl9 double mutants, unlike *cbl2 cbl3*, failed to exhibit a discernible phenotypic change on the low-K medium (Supplementary Fig. 3). This result not only indicates that these two pairs of CBLs, localized to plasma membrane and tonoplast, respectively, play distinct roles in low-K adaptation, but also verifies that the germination assay described in this study would probably identify remobilization mutants rather than mutants defective in K⁺ uptake.

We next examined the seed germination of cbl2 or cbl3 single mutants on low-K medium to dissect the functional redundancy. Although cbl3 showed slightly retarded germination on the medium with an extremely low level of K⁺ (0.01 mM), the cbl2 cbl3 double mutant displayed a much stronger phenotype (Supplementary Fig. 4). In the presence of 0.05 mM or 0.1 mM K⁺, defect in seed germination was observed only in the double mutant but not in the single mutants (Supplementary Fig. 4). Moreover, transgenic expression in the cbl2 cbl3 background of either CBL2 or CBL3 restored seed germination under low-K conditions (Supplementary Fig. 5). Taken together, these results demonstrated that CBL2 and CBL3 function redundantly in low-K adaptation in Arabidopsis.

To extend the phenotypic analysis under low-K conditions, we subjected the seedlings to postgermination growth assay on agarose plates. When grown on the low-K medium containing 0.01, 0.05 or 0.1 mM K⁺, *cbl2 cbl3* mutants grew worse than wild-type plants, with more stunted shoot and root systems (Supplementary Fig. 6).

We noted that $cbl2\ cbl3$ shows a different phenotype in an earlier study using a high concentration of ammonium (NH₄⁺) in the medium²². We thus phenotyped $cbl2\ cbl3$ on media with variable K⁺ and NH₄⁺ supplies. With low millimolar levels of NH₄⁺, $cbl2\ cbl3$ clearly displayed a low-K hypersensitive phenotype (Supplementary Fig. 7). In the presence of 20 mM NH₄⁺, however, $cbl2\ cbl3$ seedlings appeared larger and greener than the wild type (Supplementary Fig. 7), which was earlier interpreted as more 'resistant' to low-K conditions²². We therefore concluded that NH₄⁺ toxicity can mask the true phenotype of mutants under low-K conditions. Hence, we set the external NH₄⁺ at 1 mM to avoid its toxic effect.

To address the role of CBL2 and CBL3 in K⁺ homeostasis during an extended growth period, we cultured the seedlings hydroponically and examined their phenotypes for four weeks. Under a wide range of low-K conditions, *cbl2 cbl3* seedlings were consistently more stunted than wild-type plants (Supplementary Fig. 8).

A short-term K⁺-starvation treatment of mature plants may directly manifest plant capacities in the K⁺ remobilization process. We thus transferred plants from K⁺-sufficient to K⁺-deficient conditions and monitored their growth for 9 d. We found that, while wild-type plants remained healthy, *cbl2 cbl3* plants were stunted with strong chlorosis at leaf tips, a typical symptom for K⁺ deficiency in plants (Fig. 1c). Quantification of the root and shoot biomass confirmed that growth of *cbl2 cbl3* mutants was severely affected within 9 d of K⁺ deprivation (Fig. 1d).

K+ homeostasis, but not uptake, is severely impaired in the cbl2 cbl3 mutant plants. To explore the mechanism underlying CBL2/3-mediated low-K adaptation, we measured K content in wild-type and cbl2 cbl3 plants grown in different K+ regimes on agarose plates. To our surprise, although the mutant plants were extremely sensitive to low-K levels in the medium, they exhibited a significantly higher K content as compared with the wild type, particularly under low-K conditions (Fig. 2a). We then measured the K content in the adult plants from hydroponic culture. When plants were transferred from 10 mM to 0.01 mM K+, we found a dramatic drop in K accumulation in both roots and shoots of wildtype plants. Interestingly, shoot K content in cbl2 cbl3 plants was more than double of the level in wild-type plants, although K level in roots was similar between cbl2 cbl3 and the wild type (Fig. 2b). Furthermore, when grown in a wide range of external K+ concentrations (0.01, 0.1, 0.5, 1, 3 and 10 mM), cbl2 cbl3 mutant plants consistently retained a higher K content in the shoots as compared with wild-type plants (Fig. 2c).

To date, a large majority of low-K hypersensitive mutants show defects associated with root K⁺ uptake. Although the initial screen in this study was designed to identify mutants potentially defective in vacuolar K⁺ remobilization, we cannot exclude the possibility that CBL2 and CBL3 may also regulate K⁺ uptake. We compared *cbl2 cbl3* mutants with the wild-type plants in root K⁺ uptake capacity using the rubidium (Rb⁺) tracer assay⁵ and found no difference. In contrast, the well-known K⁺-uptake mutant (lacking both AKT1 and HAK5) showed severely reduced uptake rates (Fig. 2d). These results further support the conclusion that CBL2 and CBL3 regulate K⁺ homeostasis without altering K⁺ uptake in *Arabidopsis*.

To further understand the defect of K⁺ homeostasis in *cbl2 cbl3*, we monitored the expression of low-K-induced marker genes²⁵ in wild-type and mutant seedlings as a proxy for relative cytoplasmic K⁺ levels. Upon K⁺ starvation, all of the tested gene markers were expressed at higher levels in the *cbl2 cbl3* mutant than in the wild type (Supplementary Fig. 9), suggesting that *cbl2 cbl3* mutant plants were physiologically more starved of the K⁺ nutrient despite an overaccumulation of total K. These results further support the initial hypothesis that CBL2 and CBL3 may control remobilization of the vacuolar K⁺ pool. As the primary K⁺ reserve for remobilization comes from the majority of leaf cells containing large vacuoles, it is

reasonable to see that shoot K content is more affected, as compared with the root K content, in the *cbl2 cbl3* mutant.

A quartet of CIPKs partner with tonoplast Ca2+ sensors in plant low-K adaptation. It has become a widely accepted paradigm that CBL proteins physically and functionally interact with CIPKs to regulate membrane transport processes^{8,9}. To identify CIPKs involved in the CBL2/3-mediated pathway in plant low-K adaptation, we first analysed the expression levels of CIPK genes during seed germination in response to K+ deficiency. Among the 26 CIPKs in Arabidopsis, CIPK6, 9 and 25 exhibited a strong induction (>tenfold) at the transcriptional level under low-K conditions (Supplementary Fig. 10a). We examined loss-of-function mutants of cipk6, cipk9 and cipk25 under low-K conditions and found that the growth of cipk9 mutants, but not cipk6 or cipk25, was slightly arrested in the presence of 0.01 mM K⁺ (Supplementary Fig. 10b,c), suggesting that CIPK9 may function in plant adaptation to K+ starvation, consistent with the finding in a previous study26. However, the phenotypes of cipk9 single mutants were much weaker than cbl2 cbl3 when grown under low-K conditions, probably due to functional redundancy with other CIPKs. Indeed, we earlier showed that CIPK9, as well as its three close homologues CIPK3, 23 and 26, can interact with CBL2 and CBL3 in the tonoplast to regulate plant tolerance to high magnesium (Mg²⁺) stress²⁷. It is tempting to speculate the same signalling complexes in the tonoplast may also be responsible for plant low-K responses. To test this hypothesis, we created a series of multigene mutants among cipk3, 9, 23 and 26, and in particular we established a second set of combinations of independent alleles that was not available in the previous study (Supplementary Fig. 11). We subjected these genetic materials to low-K growth assays as conducted earlier for the cbl2 cbl3 mutant. We found that among all the single mutants only *cipk9* showed a discernible phenotype. The cipk9 cipk23 double mutants showed a much stronger phenotype than the cipk3 cipk26 double mutants under low-K conditions during seed germination (Fig. 3a and Supplementary Fig. 12a), as revealed by plant fresh weight (Fig. 3b and Supplementary Fig. 12b). This is interesting because our previous study indicates that the same cipk9 cipk23 mutant did not show a strong phenotype under high-Mg conditions²⁷, suggesting that these CIPKs do not contribute to the two nutrient-associated stresses (low-K versus high-Mg) in the same manner, although they partner with the same CBLs. In the hydroponic solutions containing extremely low K⁺ (0.01 mM), even single mutants of cipk9 and cipk23 exhibited mild but significant growth retardation as compared with wild type. But cipk9/23 double and cipk9/23/26 triple mutants showed much stronger defects, to a similar level as cbl2 cbl3 (Fig. 3c,d). In the presence of 0.1 mM K⁺, *cipk9* and *cipk23* single mutants became comparable with wild type, but growth defects remained strong in *cipk9/23* and cipk9/23/26 mutants (Fig. 3c,d). When analysing the various triple mutants, we found that all of them were hypersensitive to low-K conditions, although cipk3/23/26 was the weakest and cipk9/23/26 was the strongest (Supplementary Fig. 12c,d). This phenotype 'gradient' in single, double, triple mutants under different K+ regimes reflects a functional overlap among the four CIPK partners of CBL2 and CBL3 in low-K adaptation.

We also subjected various plants to the K^+ starvation treatment. In this assay, only the *cipk3/9/23/26* quadruple mutant displayed an identical phenotype to *cbl2 cbl3* among all the genetic mutants described above (Supplementary Fig. 13). The two independent alleles of *cipk3/9/23/26* quadruple mutant, like the *cbl2 cbl3* mutant, were both severely stressed with leaf tip necrosis, suggesting that these four CIPKs all function downstream of CBL2 and CBL3 in the K^+ remobilization process (Fig. 3e), although their individual contributions may differ. Among them, CIPK9 and CIPK23 may contribute more significantly than CIPK3 and CIPK26. In particular, CIPK23 appears to play a dual role in both K^+ absorption 10,24

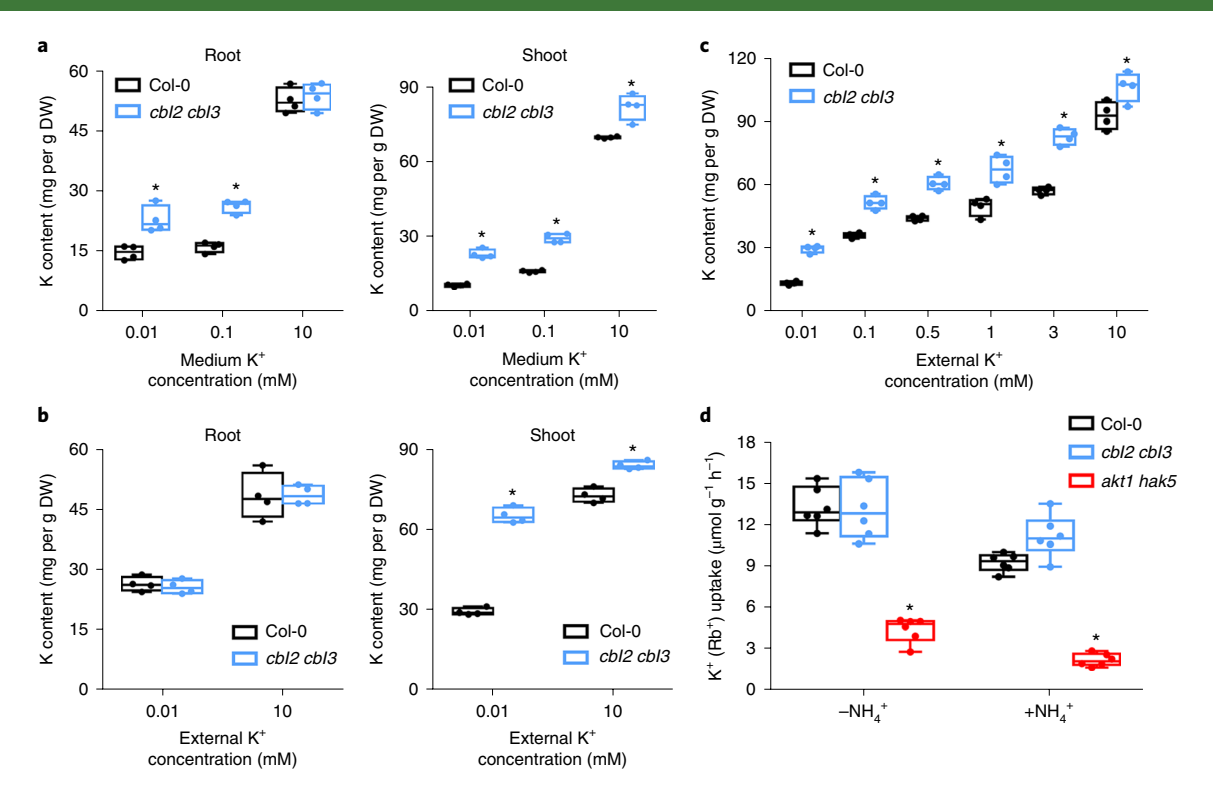


Fig. 2 | K content in the *cbl2 cbl3* **mutant. a**, K content in the root and shoot tissues of two-week-old wild-type (Col-0) and *cbl2 cbl3* plants grown on agarose plates supplemented with different concentrations of K⁺ (n=4 biological replicates). Asterisks indicate statistically significant differences between the wild type and *cbl2 cbl3* analysed by two-tailed Student's *t*-tests, *P<0.05. The exact P values are as follows: for root, from left to right, P=4.74×10⁻³, 5.22×10⁻⁵, 0.624; for shoot, from left to right, P=1.24×10⁻⁵, 7.38×10⁻⁶, 3.52×10⁻³. **b**, K content in the root and shoot tissues was measured at the end of the K⁺-starvation assay as shown in Fig. 1b (n=4 biological replicates). Asterisks indicate statistically significant differences between the wild type and *cbl2 cbl3* analysed by two-tailed Student's *t*-tests, *P<0.05. The exact P values are as follows: for root, at 0.01 and 10, P=0.555 and 0.944, respectively; for shoot, at 0.01 and 10, P=4.36×10⁻⁷ and 2.71×10⁻⁴, respectively. **c**, K content in the shoot tissue of hydroponically grown plants. Wild-type plants and *cbl2 cbl3* mutants were grown in hydroponic solutions to one-month-old stage in the presence of different K⁺ concentrations. Shoot materials were harvested for the determination of K content (n=4 biological replicates). Asterisks indicate statistically significant differences between the wild type and *cbl2 cbl3* analysed by two-tailed Student's *t*-tests, *P<0.05. The exact P values are as follows: from left to right, P=2.19×10⁻⁶, 9.51×10⁻⁵, 6.03×10⁻⁵, 3.54×10⁻³, 1.77×10⁻⁵, 0.0268. **d**, K⁺ (Rb⁺) uptake rates in the wild type, and *cbl2 cbl3* and *akt1 hak5* mutants in the absence or presence of NH₄⁺ (n=6 biological replicates). Asterisks indicate statistically significant differences analysed by two-tailed Student's *t*-tests, *P<0.05. The exact P values are as follows: for $-NH_4$ ⁺, P=0.883 (Col-0 versus *cbl2 cbl3*), P=1.53×10⁻⁷ (Col-0 versus

and remobilization, while the other three CIPKs mainly function in the latter process. This idea was supported by the finding that the *cipk3/9/26* triple mutant, like the *cbl2 cbl3* double mutant, overaccumulated K in the shoots, whereas *cipk9/23/26* and *cipk3/9/23/26* mutants did not, presumably because CIPK23 mutation additively leads to impaired K⁺ uptake (Fig. 3f).

In this study, we found that the *akt1 hak5* double mutant, lacking the two major K⁺-uptake transporters in the roots, did not display leaf necrosis, a typical K⁺ deficiency symptom shown in *cbl2 cbl3* (Supplementary Fig. 13), although K content in both roots and shoots was greatly reduced in the *akt1 hak5* mutant as compared with the wild type (Fig. 3f). Moreover, we compared the phenotypes of *cbl1 cbl9* and *cbl2 cbl3* in various low-K treatment assays, and found that *cbl2 cbl3* displayed a severe growth inhibition in all cases when K⁺ was deficient, whereas *cbl1 cbl9* failed to show a pronounced phenotype upon a short period of K⁺ starvation (Supplementary Fig. 14). These findings suggest that immediate K⁺ remobilization from vacuolar stores, rather than K⁺ uptake, serves as a predominant mechanism in coping with short-term K⁺ starvation, a condition often encountered by plants under natural conditions.

Tonoplast CBL-CIPK modules regulate the vacuole-to-cytosol **K**⁺ **transport.** Our previous study has shown that CBL2 and CBL3 form protein complexes with CIPK3, 9, 23 and 26 at the vacuolar membrane²⁷. We hypothesize that the tonoplast CBL-CIPK modules directly regulate K⁺ retrieval from the vacuolar pool to cope with K⁺ deficiency. To test this hypothesis, we examined K⁺ fluxes from the vacuole into the cytoplasm using the patch-clamp technique. In the whole-vacuole mode, instantaneous K+-permeable currents were recorded at both positive and negative voltages in the wild-type vacuoles isolated from mesophyll cells (Fig. 4a). Because pH gradient across the tonoplast under physiological conditions establishes a negative membrane potential that favours cation efflux from the vacuole²⁸, we focused on the K⁺ current detected in the range of negative test voltages. Importantly, the inward K⁺ current (from vacuolar lumen to the cytosol) physiologically corresponds to the vacuolar K⁺ remobilization process. Under the same experimental condition, vacuoles from cbl2 cbl3 mesophyll cells exhibited dramatically reduced inward K⁺ currents compared with those from wild-type plants (Fig. 4a), suggesting that vacuolar K+ remobilization was seriously impeded in the mutant. Further analysis in multiple cipk mutants showed that mutation of CIPK9 alone slightly

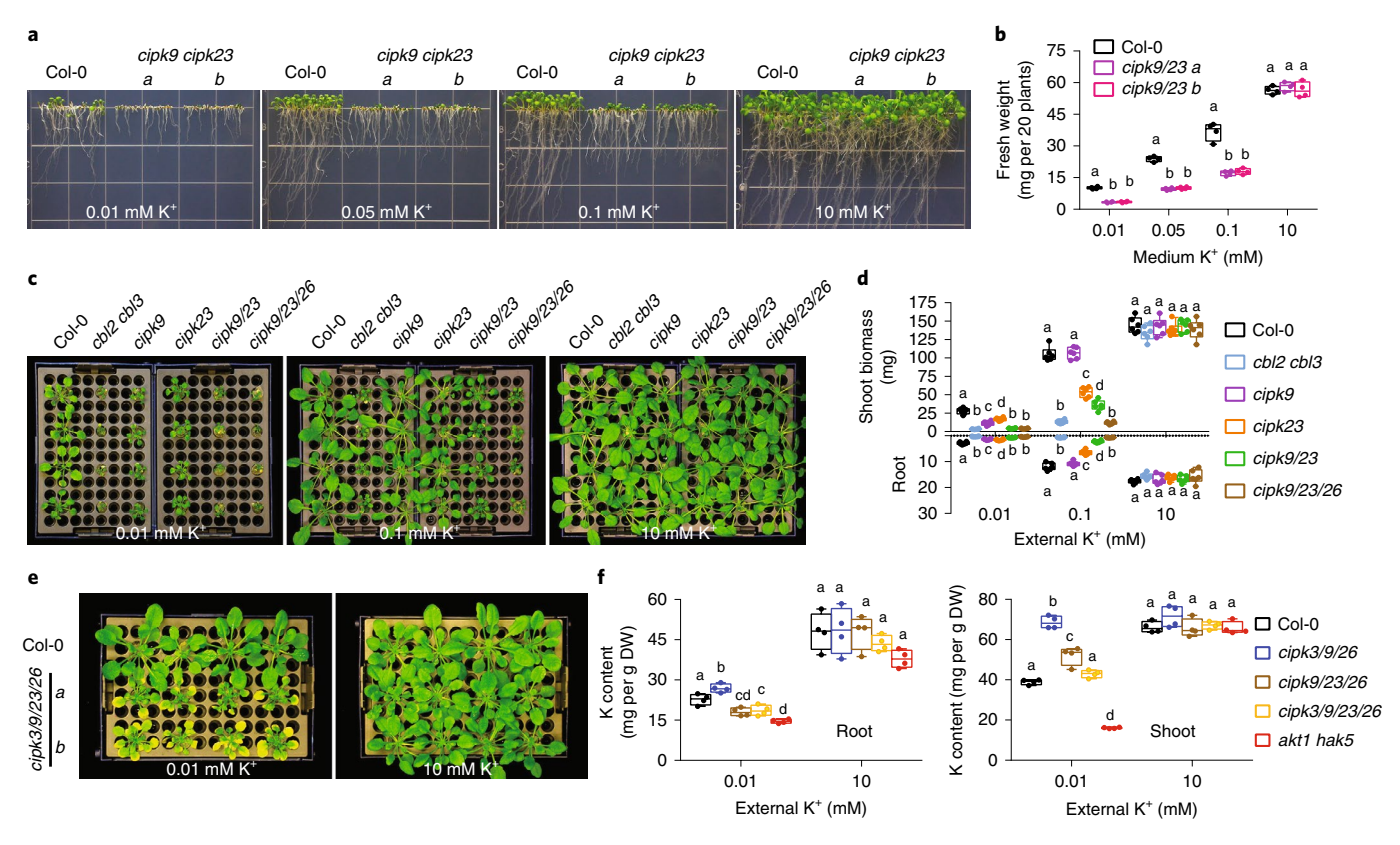


Fig. 3 | A quartet of CIPKs functions downstream of CBL2/3 in plant adaptation to low-K conditions. **a**, Seed germination of the wild type (Col-0) and two independent alleles of cipk9 cipk23 double mutants under different external K⁺ concentrations. Representative images show eight-day-old seedlings after direct germination on the K-free growth medium supplemented with indicated concentrations of KCl (n = 4 biological replicates). **b**, Measurement of seedling fresh weight (n = 4 biological replicates) at the end of the seed germination assay as shown in **a**. **c**, Growth phenotype of one-month-old wild-type plants as well as different cbl and cipk mutants in hydroponic solutions containing indicated concentrations of K⁺. Seven-day-old seedlings germinated on MS plates were transferred to hydroponic solutions for further 23-d growth. Photographs were taken on the 23rd day after the plants were grown under hydroponic conditions. Independent experiments were repeated three times. **d**, Measurement of root and shoot biomass of one-month-old plants in hydroponic solutions as shown in **c** (n = 6 biological replicates). **e**, Growth phenotype of the wild type and two independent alleles of cipk3/9/23/29 quadruple mutant during K⁺ starvation treatment. Wild-type and mutant plants were grown under K-replete conditions (10 mM K⁺) for 18 d and then transferred to new hydroponic solutions containing either insufficient K⁺ (0.01 mM) or sufficient K⁺ (10 mM) for another 9 d. Photographs were taken at the end of the nine-day treatment. Independent experiments were repeated three times. **f**, Quantification of root and shoot K content in various plant materials after the K⁺ starvation treatment. After the 9-d transfer of the 18-day-old plants to K-insufficient (0.01 mM) or K-sufficient (10 mM) solutions, root and shoot samples were collected in each genotype followed by the measurement of K content (n = 4 biological replicates). Box plots in **b**, **d**, **f** show the minimum, 25th percentile, median,

reduced vacuolar K⁺ conductance, whereas cipk23 single mutants showed no difference from the wild type (Fig. 4a). Double mutation of CIPK9 and CIPK23 substantially disrupted the activity of vacuolar K+ transport. The K+ efflux currents in triple and quadruple mutants were further compromised (Fig. 4a). Current magnitudes in cbl2 cbl3 as well as higher-order cipk mutants were quantitatively analysed in the form of a current-voltage (I-V) curve (Fig. 4b), which suggested that multiple CIPKs differentially but cooperatively contributed to the regulation of K+ efflux from the vacuolar pool, consistent with their contribution to low-K adaptation phenotype described earlier. At a test voltage of −100 mV, the current amplitude measured in cbl2 cbl3 vacuoles was only about 20% of that in the wild type (Fig. 4c). While single *cipk* mutants were slightly compromised in the vacuolar K+ conductance, higher-order cipk mutants featured a gradient of reduction in the K+ current amplitude (Fig. 4c). Most strikingly, the inward K+ current across the tonoplast in the quadruple mutant cipk3/9/23/26 was diminished to a similar level as observed in cbl2 cbl3 (Fig. 4b,c), further supporting the conclusion that these four CIPKs redundantly act downstream

of the two tonoplast Ca^{2+} sensors in regulating vacuole-to-cytosol K^+ transport.

Reconstitution of the vacuolar K+ efflux by the TPK-type channel coupled with tonoplast CBL-CIPK modules. Electrophysiological recordings of channel activities in the tonoplast have identified fast vacuolar (FV) and slow vacuolar (SV) channels, as well as vacuolar K+-selective (VK) cation channels, which may synergistically mediate vacuolar K+ release²⁹. We thus reasoned that some of these channels might be directly regulated by the tonoplast CBL-CIPK modules involved in vacuolar K⁺ remobilization. To test this hypothesis, we attempted to reconstitute the vacuolar K⁺ release pathway in a plant cell system. While the molecular nature of the FV components remains elusive and the SV channel TPC1 is multifunctional³⁰, VK currents encoded by two-pore K+s (TPKs) appear to play a more specific role in plant K+ homeostasis and nutrition³¹. We thus tested the possible link between TPK-type channels and CBL-CIPK signalling modules. After transiently expressing Arabidopsis TPK channels with or without CBL-CIPK modules

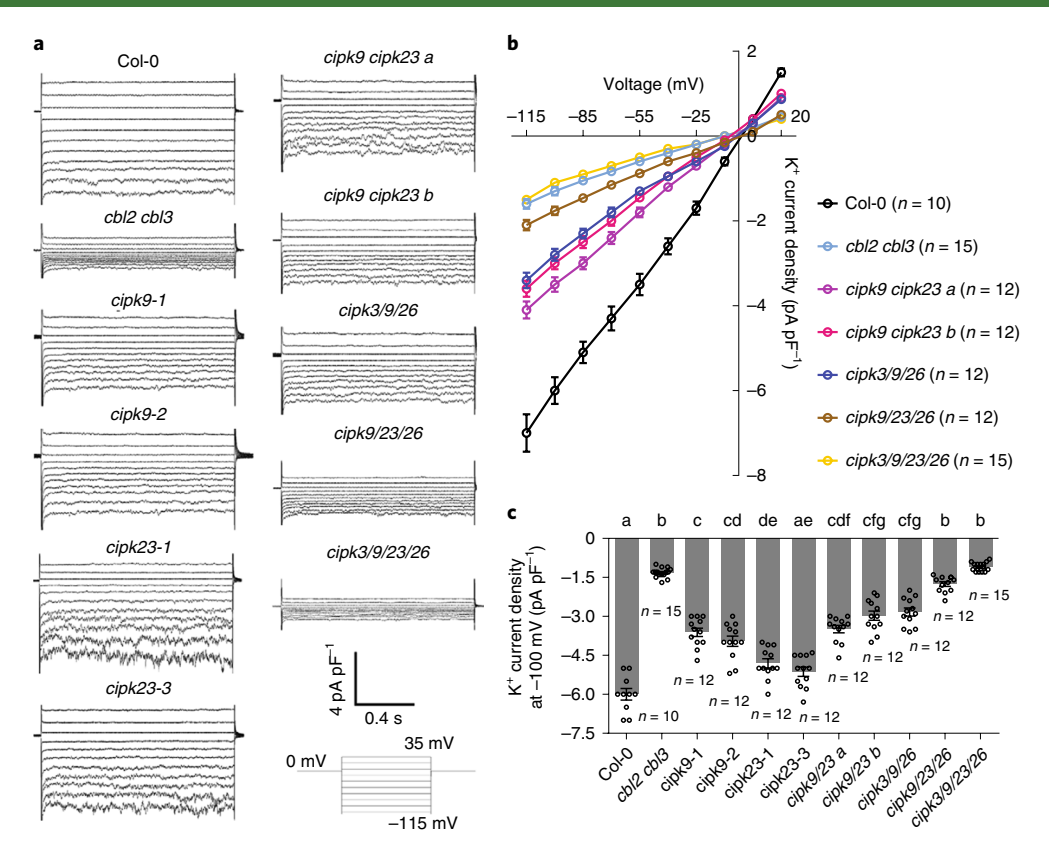


Fig. 4 | Reduced vacuolar K⁺ **inward current in various** *cbl* **and** *cipk* **mutants. a**, Whole-vacuole K⁺ current density traces of a representative vacuole from the wild type (Col-0), cbl2 cbl3 mutant and multiple *cipk* mutants as indicated. The scale of current density and elapsed time as well as the recording protocol are depicted in the bottom right panel. All the experiments were repeated at least three times. **b**, Standardized current-voltage curves of stationary current densities recorded in wild type, cbl2 cbl3 and multiple cipk mutants. Symbols and error bars denote mean and standard error; n represents independent biological samples. **c**, Quantification of the K⁺ current density across the tonoplast from different plant materials at the imposed voltage of -100 mV. Statistically significant differences between groups were analysed by one-way ANOVA followed by a Tukey's multiple comparison test. Different letters indicate significant differences at P < 0.05. Bars and error bars denote mean and standard error; n represents independent biological samples.

in Nicotiana benthamiana, we recorded the K+ current emanating from the isolated vacuoles of mesophyll cells expressing the transgenes. To better monitor the expression of each component, TPK, CBL and CIPK proteins were tagged with three different types of fluorescent proteins, VENUS, CFP and mCherry, respectively, which can be readily distinguished in a single cell³². After extensive trials, we achieved co-expression of all three components in a single mesophyll cell and all of them could be colocalized to the membrane of an isolated vacuole (Fig. 5a). When TPK1 was expressed alone, a clear inward K⁺ current across the tonoplast was recorded, which is significantly higher than the background activity (Fig. 5b). This observation indicates that, under our experimental conditions, endogenous background VK current was overshadowed by the transiently expressed TPK1 whose activity can thus be conveniently examined in this system. Compared with TPK1 alone or TPK1 co-expressed with mCherry, co-expression of CIPK9 with TPK1 resulted in a significant elevation in the channel activity and this CIPK9-induced activation was further augmented after coupling the expression of CBL3 (Fig. 5b). Compared with vacuoles expressing TPK1 alone, the CBL3-CIPK9-TPK1 co-expression induced a threefold larger current (Fig. 5c). On the other hand, the kinasedead version of CIPK9 harbouring a Lys-to-Asn mutation³³ failed to amplify TPK1 current (Fig. 5b), indicating that the kinase activity of CIPK9 is indispensable for the channel activation. Besides, the CBL3-CIPK9 module only marginally activated the endogenous VK channels in the absence of TPK1 (Fig. 5b,c), validating that the

exogenous components CBL3, CIPK9 and TPK1 constitute a linear pathway that facilitates K+ release from Arabidopsis vacuoles. To further confirm the observed vacuolar currents were carried by K+, we applied various concentrations of K⁺ in the bath solution (cytosolic side of tonoplast) and found that the TPK1 currents were highly dependent on cytosolic K⁺ concentration (Supplementary Fig. 15). The reversal potentials (E_{rev}) were shifted to more positive values with decreasing cytosolic K+ concentrations, which correlated well with the predicted Nernst K⁺ equilibrium potentials (E_{Nernst}), indicating that the recorded currents are mediated by K⁺ movement. We next conducted experiments involving two other members of TPK family channels targeted to the tonoplast34,35 and found that both TPK3 and TPK5 could also be activated by CBL3-CIPK9 in a similar manner (Supplementary Fig. 16), implicating CBL-CIPK activation as a universal regulatory mechanism for TPK-type channels. Furthermore, co-expression of CBL3 in combination with CIPK3, CIPK23 or CIPK26, but not with CIPK24, enhanced TPK1-elicited current as well (Supplementary Fig. 17), which is consistent with the genetic redundancy of the four CIPK members. The specificity of TPK1 regulation by CBL-CIPK modules was also addressed using different CBLs. Unlike the tonoplast-localized CBL2 and CBL3, CBL1 that resides in the plasma membrane failed to further activate the TPK1 channel on top of CIPK9 (Supplementary Fig. 18). In addition, Ca²⁺ was required for CBL-CIPK activation of the TPK1 channel, as adding Ca2+ chelator EGTA to the bath solution (cytoplasmic side) entirely abolished the channel activity while

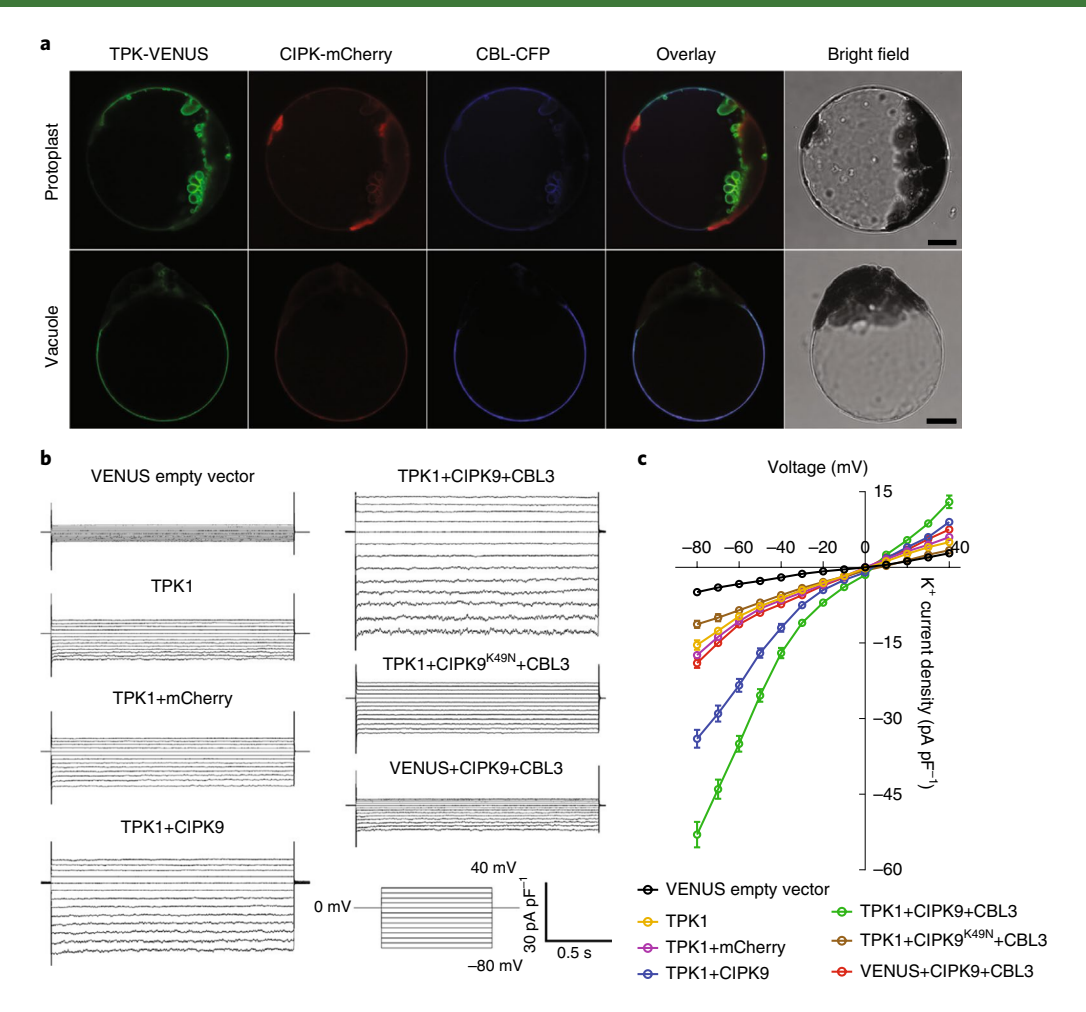


Fig. 5 | Reconstitution of the vacuolar K⁺ **efflux pathway consisting of TPK channels and CBL-CIPK modules. a**, Co-expression of the TPK channel and CBL-CIPK module in a single plant cell as well as an isolated vacuole. Confocal laser scanning microscopy images of a typical mesophyll protoplast and an isolated vacuole transiently expressing the three components tagged with three distinct types of fluorescent proteins. The VENUS, mCherry and CFP signals were labelled green, red and blue, respectively. Scale bars, 10 μm. Images are representative from ten independent biological samples. **b**, Typical K⁺ current density traces recorded across the vacuole membrane of plant cells co-expressing indicated combinations of TPK, CBL and CIPK. Bottom right inset illustrates the protocol and the scale of the recordings in patch-clamp experiments. All the experiments were repeated three times. **c**, Current-voltage curves of stationary currents recorded in the experiments as shown in **b**. Symbols and error bars denote mean and standard error. For the group of TPK1–CIPK9^{K48N}–CBL3, n = 8; for all the other combinations, n = 10.

submillimolar levels of Ca^{2+} maintained the activation of TPK1 by CBL3–CIPK9 (Supplementary Fig. 19). Taken together, these results reconstituted a vacuolar Ca^{2+} -dependent CBL–CIPK pathway modulating the activity of TPK-type K^+ channels that may function in vacuolar K^+ release in response to K^+ deficiency.

Discussion

Acquisition of K⁺ from the external environment and K⁺ retrieval from the internal stores provide two important routes for K⁺ homeostasis in plant cells^{19,20}. As the plant vacuole serves as a major organelle for accumulation and storage of K⁺, massive K⁺ retrieval from vacuoles may occur in plants to respond to diverse environmental changes and developmental cues. One critical circumstance is when plants encounter K⁺ deficiency in the soil, which would promote K⁺ mobilization from the vacuolar pool to support the metabolic processes in the cytoplasm. A previous study indicates that, under varying extracellular K⁺ status, vacuolar K⁺ levels change rapidly whereas cytosolic K⁺ is maintained at a more constant level, supporting a model that plant cells maintain steady cytoplasmic K⁺ levels at the expense of altering the vacuolar K⁺ pool³⁶. Despite the importance of this vacuole-to-cytoplasm pathway for

 K^+ homeostasis, molecular components constituting the vacuolar K^+ release and its regulation remain largely unknown. In this study, we demonstrated that the K^+ remobilization process is activated by a Ca²+-dependent CBL–CIPK signalling network, which serves as a critical mechanism for plants to cope with low-K stress. During K^+ starvation, tonoplast-localized Ca²+ sensors CBL2 and CBL3 physically and functionally interact with a quartet of CIPK-type kinases, which in turn activate K^+ efflux from the vacuoles, delivering the K^+ nutrient to the cytoplasm.

Several types of K⁺-permeable channels in the tonoplast are known to facilitate K⁺ release from the vacuole^{29,37}, but it remains unknown how these channels fine-tune their activity in response to the cellular K⁺ status. The vacuolar CBL–CIPK network identified in this study provides a molecular link between channel activity and cytosolic K⁺ level to adjust channel activities depending on cellular K⁺ status. To identify the effector proteins subjected to direct regulation by the CBL–CIPK modules in the tonoplast, we reconstituted the vacuolar CBL–CIPK–TPK pathway that generates a robust and well-defined inward K⁺ current mediating K⁺ efflux from the vacuolar lumen. This is consistent with the proposed function of TPK channels in plant K⁺ nutrition³¹. We speculate that other

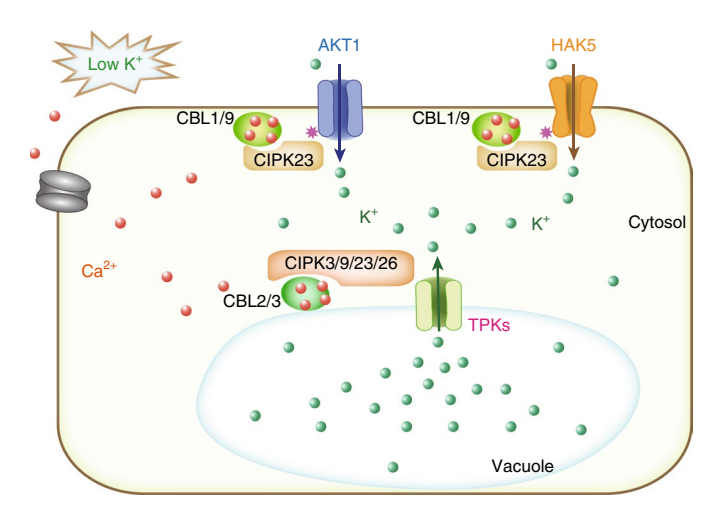


Fig. 6 | A working model depicting dual CBL-CIPK pathways in plant low-K response. Under low-K stress conditions, unidentified Ca^{2+} channels mediate Ca^{2+} influx, triggering a Ca^{2+} elevation. A pair of Ca^{2+} sensors, CBL1 and CBL9, interacts with CIPK23 and recruits CBL1/9-CIPK23 complexes to the plasma membrane where they phosphorylate and activate AKT1 and HAK5 to boost K^+ uptake. In parallel, the tonoplast-localized CBL2 and CBL3 interact with four CIPKs that, in turn, propel K^+ remobilization from the vacuole store through activating TPK-type K^+ channels. The two pathways work synergistically to ensure increased K^+ availability in the cytoplasm when external K^+ becomes limited. Red spheres denote Ca^{2+} ; green spheres denote K^+ ; purple asterisks indicate protein phosphorylation. Arrows point in the direction of K^+ flows.

tonoplast K⁺ transporters in addition to TPKs may also serve as the targets of vacuolar CBL-CIPK complexes and function synergistically with TPKs in facilitating the overall K+ efflux from vacuoles. This hypothesis resembles the scenario at the plasma membrane where CBL1/9-CIPK23 simultaneously activates two distinct types of K+ transport proteins to enhance K+ uptake under low-K conditions¹⁰⁻¹⁴. Indeed, a more recent study showed that the SV channel TPC1 and TPK1/TPK3 channels in the tonoplast act in concert to confer electrical excitability of plant vacuoles³⁸. As TPC1 is permeable to monovalent cations including K⁺ (ref. ³⁰), it may also play a role in the vacuolar K⁺ remobilization process, and hence may possibly serve as an alternative target for the vacuolar CBL-CIPK modules. As vacuolar CBL-CIPK modules and tonoplast K+ channels are evolutionarily conserved from moss to higher plants^{39,40}, Ca²⁺signalling-mediated vacuolar K+ remobilization may be a universal mechanism for land plants to respond and adapt to low-K environments. Given the pivotal roles of K+ transport in plant cell physiology, this Ca²⁺-dependent vacuolar K⁺ remobilization pathway may govern a number of diverse cellular processes, such as stomatal movement and polarized cell growth during root hair and pollen tube elongation, which warrant future studies. The dual CBL-CIPK pathways in low-K responses may preferentially function in different plant tissues depending on their expression pattern and target transporters. The plasma membrane CBL-CIPK pathway directly phosphorylates AKT1 and HAK5 that are mainly expressed in roots for K+ uptake. The vacuolar CBL-CIPK modules may be more important in shoot tissues since large amounts of K⁺ are stored in the vacuoles of mesophyll cells and serve as a major K⁺ source for remobilization. This is consistent with the expression pattern of CIPK members in the two pathways: for example, CIPK23 is highly expressed in root hairs and cortex cells²⁴ whereas CIPK9 is predominantly expressed in the shoot tissues²⁶. It is also interesting to point out that CIPK9 may function exclusively in vacuolar K+ remobilization whereas CIPK23 appears to play a dual role in both pathways. This further validates a general theme in versatility

of CIPK functions: one CIPK may interact with multiple CBLs that recruit it either to the plasma membrane or to the tonoplast where the distinct CBL–CIPK complexes regulate specific target proteins and biological processes. Another example of such versatility is provided by CIPK24/SOS2 that is recruited to the plasma membrane and tonoplast, respectively, by CBL4 and CBL10 to regulate sodium (Na⁺) exclusion or sequestration in plant salt responses^{8,41}.

It is important to note that mutants lacking the vacuolar CBL-CIPK pathway, such as cbl2 cbl3 and cipk3/9/23/26, displayed severe growth defects in a broad range of external K+ regimes. In contrast, mutants lacking the plasma membrane CBL-CIPK pathway consistently show much weaker growth phenotype under the same conditions (Supplementary Fig. 14). These data indicate that the vacuolar CBL2/3-CIPK pathway for K+ remobilization may serve as a primary mechanism for plants to respond and adapt to K+ deficiency, which appears to be more critical than the plasma membrane CBL1/9-CIPK23 pathway functioning in K⁺ uptake. Beside the fact that the vacuolar pool provides a readily available K⁺ source, vacuolar membrane potential (around +30 mV)²⁸ may constantly adjust K⁺ gradient between the vacuolar lumen and the cytosol, providing a more effective mechanism to deal with the K+ shortage in the cytosol, particularly in response to a short-term K⁺ deficiency. Nevertheless, maintaining K+ homeostasis under K+ deficiency not only involves K+ fluxes at the cellular level but also requires longdistance transport at the whole-plant level^{4,20}. Effective translocation of K⁺ from source to sink tissues relies on cooperative actions of both plasma membrane and tonoplast K+ transport systems in different cell types, which should be highly coordinated, and the dual CBL-CIPK networks provide such a regulatory mechanism to orchestrate K+ transport along the path (Fig. 6).

Ca2+ is an evolutionarily conserved and functionally versatile signalling agent in many regulatory pathways. In Arabidopsis roots, it has been shown that K+ starvation triggers two successive and distinct Ca²⁺ signals⁴². It is possible that these Ca²⁺ spikes lead to distinct downstream responses in different cell types⁴². Intriguingly, two Ca²⁺-dependent CBL-CIPK pathways also operate at different subcellular locations during plant K+ deficiency. Although it is unknown whether these two CBL-CIPK pathways are activated by distinct Ca2+ signals, they certainly target specific ion channels and regulate different K+ transport processes in the plasma membrane and vacuolar membrane, respectively. A critical feature of the CBL-CIPK signalling machinery concerns the pivotal role of Ca²⁺. In the plasma membrane pathway, efficient activation of the K+ channel AKT1 by CBL1-CIPK23 is tightly regulated by Ca²⁺ (refs. ^{11,42}). In this study, activation of vacuolar K+ efflux channels by CBL-CIPK modules is Ca²⁺-dependent as well. It is noteworthy that TPK-type channels contain putative EF-hands in their C-terminal regions and require Ca²⁺ for their channel activity^{38,43,44}. Our work here indicates that Ca²⁺ alone, without CBL-CIPK components, was not sufficient to activate TPKs beyond the basal level. It is thus possible that the resting Ca²⁺ levels in the plant cell may be a prerequisite for the basal activity and a robust Ca2+ burst induced by nutrient deficiency may be required for the further activation by the CBL-CIPK signalling pathway. A future challenge is to identify the elusive Ca2+ channels and molecular regulators responsible for generating the Ca2+ signatures in plant responses to K+ deficiency and other nutrient signals, as exemplified by recent studies^{45,46}.

Methods

Plant materials and general growth conditions. All the wild-type, mutant and transgenic *Arabidopsis* lines used in this study are Columbia (Col) ecotype. Based on the germination assay described thereinafter, we initially screened 54 homozygous *Arabidopsis* T-DNA insertion mutants defective in putative K⁺ channels and transporters or potential regulators, which include the stocks as follows: *akt1* (SALK_071803)¹⁰, *hak5* (SALK_130604), *akt1 hak5*, *kup1* (SALK_051343), *kup3* (SALK_002622), *kup4* (SALK_150351; SALK_086060), *kup5* (SALK_120707; SALK_072850), *kup7* (SALL_105_G04; GK_665A02;

SALK_206158), kup9 (SALK_108080), kup10 (GK_692H04; GK_797C11), kup11 (SAIL_203_C07; GK_625B10), kup12 (SALK_045392; SALK_083613; SALK_121784), nhx1 nhx2 (ref. 17), nhx3 (SALK_082277), kea4 (SALK_012925; SALK_008276), kea5 (SALK_140807; SALK_082203), kea6 (SALK_141501; SALK_106751), kea4 kea5 kea6 (two independent alleles)47, kc1 (SALK_116451; SALK_140579), skor (SALK_097435; GK_391G02), tpc1 (SALK_145413; GK_685C03), tpk1 (WiscDsLox385A07; SALK_146903), vha-a2 a3 (ref. 23), avp1 (GK_569C07), cbl1 cbl9 (ref. 10), cbl2 cbl3 (ref. 22), cbl4 (SALK_113101), cbl8 (SALK_083553), cbl10 (SALK_056042), cipk23-1 (SALK_032341)24, cipk9-1 (SAIL_252_F06)²⁶, cipk9-2 (SALK_058629)²⁶, cipk9-3 (SALK_014699), cipk6-1 (GK_448C12), cipk6-2 (SM_3_19294), cipk25-1 (SALK_059092), cipk25-2 (SALK_079011) and cipk25-3 (SALK_029271). In the subsequent experiments, a group of cipk mutants was employed as described in a previous study²⁷ and suffixed with 'a' in this study. Another independent set of cipk mutants harbouring T-DNA insertions was isolated in this study as follows: cipk3-1 (SALK_064491), cipk9-1 (SAIL_252_F06), cipk23-1 (SALK_032341) and cipk26-1 (SALK_005859). These single mutants as well as the higher-order mutants generating from them were suffixed with 'b'. All the higher-order mutants were generated by genetic crosses followed by identification of homozygous mutant plants from F2 or F3 progeny using PCR-based genotyping. Arabidopsis seeds were surface-sterilized and sown on solidified Murashige and Skoog (MS) medium⁴⁸. After stratification at 4°C for 2 d, the Petri dishes were placed at 22 °C for 7 d. One-week-old seedlings were transferred into the soil for subsequent growth at 22 °C in a growth chamber with a short-day (8h light and 16h dark) photoperiod or in the greenhouse under a longday (16h light and 8h dark) photoperiodic condition.

Phenotyping the growth of Arabidopsis seedlings under different K+ regimes.

For the germination assay, seeds were surface-sterilized with 0.5% sodium hypochlorite for 5 min, washed three times with water and sown on doubledistilled water supplemented with 0.25% sucrose as well as 0.8% Phytoblend (Caisson Laboratories) for solidification, or on the growth medium solidified with 0.8% agarose (Thomas Scientific). The recipe of the growth medium was modified from MS medium with a reduced level of NH₄+ optimal for seed germination and seedling growth under low-K conditions, which contained the following components: 3 mM Ca(NO₃)₂, 1.25 mM NH₄H₂PO₄, 1.5 mM MgSO₄, 0.1 mM FeSO4, 0.1 mM Na,-EDTA, 0.1 mM MnSO₄, 0.03 mM ZnSO₄, 0.1 mM H₃BO₄, $5\,\mu M$ NaI, $1\,\mu M$ Na₂MoO₄, $0.1\,\mu M$ CuSO₄, $0.1\,\mu M$ CoCl₂, 0.01% inositol and 2%sucrose. The pH of the medium was adjusted to 5.8 using NaOH and the final K+ concentration in the growth medium was adjusted by adding KCl as the K+ source. For the postgemmation assay, seeds were germinated on MS medium and grown to a four-day-old seedling stage. The seedlings were then transferred onto various agarose-solidified growth medium supplemented with different concentrations of K⁺ for subsequent growth under 80 µmol m⁻² s⁻¹ light intensity with a 12 h light and 12 h dark photoperiod. For phenotypic assay in the hydroponics, seven-dayold seedlings were transferred to the liquid solution containing 1.4 mM Ca(NO₃)₂, 0.1 mM Ca(H₂PO₄)₂, 0.125 mM MgSO₄, 0.025 mM MgCl₂, as well as 1/6 strength of MS minor salts and supplemented with different concentrations of KCl. All the hydroponic solutions for plant growth were replaced with fresh ones twice a week. For the K⁺ starvation assay, seedlings were first grown in the K-replete hydroponic solution containing 10 mM KCl for 16 d and then transferred to a new hydroponic solution containing 0.01 mM KCl for starvation for 9 d.

K content measurement and K⁺-uptake assay. To determine the K content in different tissues, plant samples were harvested separately from the root and shoot tissues at the end of each phenotypic assay, and surface-washed with double-distilled water for 15 s. The samples were then thoroughly dried in the oven at 80 °C. The dry matters were collected in a 15 ml tube and digested with 1 ml ultrapure HNO₃ (Sigma-Aldrich) in the water bath at 99 °C for 6 h. Digested samples were diluted to the appropriate concentrations with double-distilled water, and the K⁺levels in the solutions were determined by inductively coupled plasma optical emission spectroscopy (ICP-OES; PerkinElmer). Root K⁺-uptake assay was performed using Rb⁺ as a tracer, as described in previous studies^{5,12}.

RNA isolation, RT-PCR and qrt-PCR analysis. Arabidopsis seedlings grown under different conditions were harvested and ground to fine powder in liquid nitrogen. Total RNA was extracted using the TRIZOL reagent (Invitrogen) following the manufacturer's instruction. After being treated with DNase I (Invitrogen) to remove potential DNA contamination, complementary DNA was synthesized from RNA samples at 42 °C using SuperScript II reverse transcriptase (Invitrogen). The resulting cDNA products were used for PCR amplification with the gene-specific primers. Quantitative real-time PCR analysis was performed on the DNA Engine Opticon System (MJ Research) using the SYBR Green Realtime PCR Master Mix (Bio-Rad) to monitor double-stranded DNA products. Quantitative data were calculated based on the comparative threshold cycle method. The relative expression of each gene was double-normalized against the expression level of the housekeeping gene ACTIN2 and the value of gene expression measured in the wild type under K-replete conditions. All the primers used in PCR with reverse transcription (RT-PCR) and quantitative real-time PCR (qrtPCR) are listed in Supplementary Table 1.

Western blot. Plant total protein was extracted from *Arabidopsis* seedlings by grinding 100 mg of tissue in 0.3 ml of extraction buffer (50 mM Tris-HCl, pH 7.5, 5% SDS, 2% β -mercaptoethanol, 2 mM EDTA and 0.1% PMSF) in liquid nitrogen. A 5-µg sample of total protein was separated on 12% SDS–PAGE gel and electroblotted onto a nitrocellulose membrane. After being incubated with 5% milk to block non-specific binding, the membrane was probed with a rabbit anti-CBL3 polyclonal antibody or a rabbit anti-AtpA polyclonal antibody. IgG conjugated to horseradish peroxidase was used as a secondary antibody. The blot was finally visualized using the enhanced chemiluminescence immune-detection procedure.

Transient expression in Nicotiana benthamiana and protein subcellular localization. The coding sequence of each gene was in-frame fused with the indicated fluorescence protein sequence under the control of Arabidopsis ubiquitin10 gene promoter. The plant expression constructs were generated on the backbone of pCambia 1301 and transformed into the Agrobacterium tumefaciens GV3101 strain. For plant transient expression, different combinations of Agrobacterium strains carrying various constructs were co-infiltrated into the leaves of Nicotiana benthamiana in the presence of p19, a viral gene silencing suppressor. Three days after infiltration, protoplasts were isolated with the enzyme solution containing 0.4M mannitol, 20 mM MES-K (pH 5.7), 10 mM CaCl₂, 5 mM β-mercaptoethanol, 0.1% BSA, 1% cellulase R10 (Yakult Honsha, Tokyo, Japan) and 0.3% macerozyme R10 (Yakult Honsha, Tokyo, Japan). Fluorescence in the protoplasts was imaged with a confocal laser scanning microscope (LSM710, Carl Zeiss). For excitation and emission of each type of fluorescence proteins, the following filter settings are used: CFP at excitation 458 nm and emission 470-500 nm; VENUS at excitation 514 nm and emission 535-600 nm; and mCherry at excitation 561 nm and emission 580-630 nm.

Patch-clamp procedure with mesophyll vacuoles. Patch-clamp experiments were performed as described in a previous study, with some modifications³³. For patchclamp recording in Nicotiana benthamiana, vacuoles were released from isolated protoplast by mechanically rupturing the plasma membrane of selected protoplasts. More specifically, upon clamping a protoplast by the patch-microelectrode, we first applied a suction pulse to the electrode filled with bath solution. After the cell was tightly sealed, the patch-electrode was withdrawn quickly from the plasma membrane, breaking the protoplast and releasing the vacuole. A new patch-pipette was replaced to form a gigaseal contact with the vacuolar membrane, followed by electrical current recording. For patch-clamp recording in Arabidopsis, young rosette leaves from fourweek-old Arabidopsis plants were used for vacuole isolation. After being peeled for the lower epidermis, the leaves were incubated in the enzyme solution containing 1% (w/v) cellulase R10 (Yakult Honsha), 0.5% (w/v) macerozyme R10 (Yakult Honsha), 0.2% (w/v) bovine serum albumin (Sigma-Aldrich), 1 mM CaCl₂, 10 mM HEPES/Tris (pH 7.1) with an osmolarity adjusted to 500 mOsm with sorbitol. After incubation of 2h at room temperature with gentle shaking, the protoplast suspension was filtered through a 50- μm nylon mesh, followed by centrifugation at 100 g for 5 min. The pelleted protoplasts were then resuspended in 400 mM sorbitol and 1 mM CaCl₂, and vacuoles were released by applying a suction pulse to a selected protoplast with a patch-microelectrode. Whole-vacuole K+ currents were recorded using the standard patch-clamp procedure with the Axon Multiclamp 700B Amplifier (Molecular Devices). Patch pipettes were prepared from borosilicate glass capillaries (Sutter Instrument) with a P-97 puller and fire-polished to a final tip resistance of $5\,\mathrm{M}\Omega$. The bath solution (cytosolic side) contained: (1) 99 mM potassium glutamate, 1 mM KCl, 1 mM MgCl, and 5 mM HEPES (pH 7.0), and for all the experiments in Nicotiana benthamiana CaCl, was added to 1 mM, unless otherwise specified: (2) 99 mM potassium glutamate, 1 mM KCl, 6.7 mM EGTA-5.864 mM CaCl₂ (free Ca²⁺ was set to 2 µM), 1 mM MgCl₂ and 5 mM HEPES (pH 7.0), for patch-clamp recording on vacuoles from Arabidopsis materials. The pipette solution (vacuolar side) contained: 99 mM potassium glutamate, 1 mM KCl, 1 mM CaCl₂, 1 mM MgCl₂ and 5 mM MES, adjusted to pH 5.8 with glutamic acid. The osmolarity of the bath and pipette solution was adjusted to 500 mOsm and 560 mOsm, respectively, by addition of D-sorbitol. To equilibrate the vacuolar lumen with the pipette solution, recordings were initiated 15 min after break-in. Digital low-pass filtering of currents was performed at a cut-off frequency of 2.9 kHz. According to the convention of electrical recording of ionic fluxes across an endomembrane, negative currents correspond to cations moving from the vacuolar lumen into the cytoplasmic side. Steady-state currents were calculated by averaging the last 100 ms of each current trace. Raw currents were normalized into current densities ($pA\,pF^{-1}$) to offset the variations in the tonoplast capacitance of each vacuole. Current-voltage (I-V) relationships were obtained by plotting current densities against the applied test voltages.

Reporting Summary. Further information on the research design is available in the Nature Research Reporting Summary linked to this article.

Data availability

All the data supporting the findings of this study are available within the article and its Supplementary Information files or from the corresponding author upon reasonable request.

Received: 2 September 2019; Accepted: 17 February 2020; Published online: 30 March 2020

References

- Luan, S., Lan, W. Z. & Lee, S. C. Potassium nutrition, sodium toxicity, and calcium signaling: connections through the CBL-CIPK network. *Curr. Opin. Plant Biol.* 12, 339–346 (2009).
- Maathuis, F. J. M. Physiological functions of mineral macronutrients. Curr. Opin. Plant Biol. 12, 250–258 (2009).
- Ashley, M. K., Grant, M. & Grabov, A. Plant responses to potassium deficiencies: a role for potassium transport proteins. *J. Exp. Bot.* 57, 425–436 (2006).
- Wang, Y. & Wu, W. H. Potassium transport and signaling in higher plants. *Annu. Rev. Plant Biol.* 64, 451–476 (2013).
- Rubio, F., Aleman, F., Nieves-Cordones, M. & Martinez, V. Studies on Arabidopsis athak5, atakt1 double mutants disclose the range of concentrations at which AtHAK5, AtAKT1 and unknown systems mediate K⁺ uptake. Physiol. Plant. 139, 220–228 (2010).
- Aleman, F., Nieves-Cordones, M., Martinez, V. & Rubio, F. Root K⁺ acquisition in plants: the *Arabidopsis thaliana* model. *Plant Cell Physiol.* 52, 1603–1612 (2011).
- Pyo, Y. J., Gierth, M., Schroeder, J. I. & Cho, M. H. High-affinity K⁺ transport in *Arabidopsis*: AtHAK5 and AKT1 are vital for seedling establishment and postgermination growth under low-potassium conditions. *Plant Physiol.* 153, 863–875 (2010).
- 8. Luan, S. The CBL-CIPK network in plant calcium signaling. *Trends Plant Sci.* **14**, 37–42 (2009).
- Tang, R. J., Wang, C., Li, K. & Luan, S. The CBL-CIPK calcium signaling network: unified paradigm from 20 years of discoveries. *Trends Plant Sci.* (in the press).
- 10. Xu, J. et al. A protein kinase, interacting with two calcineurin B-like proteins, regulates K+ transporter AKT1 in *Arabidopsis*. *Cell* **125**, 1347–1360 (2006).
- Li, L. G., Kim, B. G., Cheong, Y. H., Pandey, G. K. & Luan, S. A Ca²⁺ signaling pathway regulates a K⁺ channel for low-K response in *Arabidopsis*. *Proc. Natl Acad. Sci. USA* 103, 12625–12630 (2006).
- 12. Ragel, P. et al. The CBL-interacting protein kinase CIPK23 regulates HAK5-mediated high-affinity K⁺ uptake in *Arabidopsis* roots. *Plant Physiol.* **169**, 2863–2873 (2015).
- 13. Li, J. et al. The Os-AKT1 channel is critical for K^+ uptake in rice roots and is modulated by the rice CBL1-CIPK23 complex. Plant Cell **26**, 3387–3402 (2014).
- Scherzer, S. et al. Calcium sensor kinase activates potassium uptake systems in gland cells of Venus flytraps. Proc. Natl Acad. Sci. USA 112, 7309-7314 (2015).
- Gaymard, F. et al. Identification and disruption of a plant shaker-like outward channel involved in K⁺ release into the xylem sap. Cell 94, 647–655 (1998).
- Very, A. A. & Sentenac, H. Molecular mechanisms and regulation of K⁺ transport in higher plants. Annu. Rev. Plant Biol. 54, 575–603 (2003).
- Bassil, E. et al. The Arabidopsis Na⁺/H⁺ antiporters NHX1 and NHX2 control vacuolar pH and K⁺ homeostasis to regulate growth, flower development, and reproduction. Plant Cell 23, 3482–3497 (2011).
- Barragan, V. et al. Ion exchangers NHX1 and NHX2 mediate active potassium uptake into vacuoles to regulate cell turgor and stomatal function in *Arabidopsis. Plant Cell* 24, 1127–1142 (2012).
- Cherel, I., Lefoulon, C., Boeglin, M. & Sentenac, H. Molecular mechanisms involved in plant adaptation to low K⁺ availability. *J. Exp. Bot.* 65, 833–848 (2014).
- Amtmann, A. & Armengaud, P. The role of calcium sensor-interacting protein kinases in plant adaptation to potassium-deficiency: new answers to old questions. Cell Res. 17, 483–485 (2007).
- Moussavi-Nik, M. P. J., Hollamby, G. J. & Graham, R. D. Dynamics of nutrient remobilization during germination and early seedling development in wheat. J. Plant Nutr. 21, 421–434 (1998).
- Tang, R. J. et al. Tonoplast calcium sensors CBL2 and CBL3 control plant growth and ion homeostasis through regulating V-ATPase activity in *Arabidopsis*. Cell Res. 22, 1650–1665 (2012).
- Krebs, M. et al. Arabidopsis V-ATPase activity at the tonoplast is required for efficient nutrient storage but not for sodium accumulation. Proc. Natl Acad. Sci. USA 107, 3251–3256 (2010).
- 24. Cheong, Y. H. et al. Two calcineurin B-like calcium sensors, interacting with protein kinase CIPK23, regulate leaf transpiration and root potassium uptake in *Arabidopsis. Plant J.* **52**, 223–239 (2007).
- Armengaud, P., Breitling, R. & Amtmann, A. The potassium-dependent transcriptome of *Arabidopsis* reveals a prominent role of jasmonic acid in nutrient signaling. *Plant Physiol.* 136, 2556–2576 (2004).
- Pandey, G. K. et al. CIPK9: a calcium sensor-interacting protein kinase required for low-potassium tolerance in *Arabidopsis. Cell Res.* 17, 411–421 (2007).
- Tang, R. J. et al. Tonoplast CBL-CIPK calcium signaling network regulates magnesium homeostasis in *Arabidopsis. Proc. Natl Acad. Sci. USA* 112, 3134–3139 (2015).
- Sze, H., Li, X. H. & Palmgren, M. G. Energization of plant cell membranes by H⁺-pumping ATPases: regulation and biosynthesis. *Plant Cell* 11, 677–689 (1999).
- 29. Hedrich, R. Ion channels in plants. Physiol. Rev. 92, 1777-1811 (2012).

- Hedrich, R., Mueller, T. D., Becker, D. & Marten, I. Structure and function of TPC1 vacuole SV channel gains shape. Mol. Plant 11, 764–775 (2018).
- Gobert, A., Isayenkov, S., Voelker, C., Czempinski, K. & Maathuis, F. J. The two-pore channel *TPK1* gene encodes the vacuolar K⁺ conductance and plays a role in K⁺ homeostasis. *Proc. Natl Acad. Sci. USA* 104, 10726–10731 (2007).
- 32. Shaner, N. C., Steinbach, P. A. & Tsien, R. Y. A guide to choosing fluorescent proteins. *Nat. Methods* 2, 905–909 (2005).
- Zhang, H. W. et al. Two tonoplast MATE proteins function as turgorregulating chloride channels in *Arabidopsis. Proc. Natl Acad. Sci. USA* 114, E2036–E2045 (2017).
- Voelker, C., Schmidt, D., Mueller-Roeber, B. & Czempinski, K. Members of the *Arabidopsis* AtTPK/KCO family form homomeric vacuolar channels in planta. Plant J. 48, 296–306 (2006).
- Hohner, R. et al. Photosynthesis in Arabidopsis is unaffected by the function of the vacuolar K⁺ channel TPK3. Plant Physiol. 180, 1322–1335 (2019).
- Walker, D. J., Leigh, R. A. & Miller, A. J. Potassium homeostasis in vacuolate plant cells. Proc. Natl Acad. Sci. USA 93, 10510–10514 (1996).
- Martinoia, E. Vacuolar transporters—companions on a longtime journey. Plant Physiol. 176, 1384–1407 (2018).
- Jaslan, D. et al. Voltage-dependent gating of SV channel TPC1 confers vacuole excitability. Nat. Commun. 10, 2659 (2019).
- Kleist, T. J., Spencley, A. L. & Luan, S. Comparative phylogenomics of the CBL-CIPK calcium-decoding network in the moss *Physcomitrella*, *Arabidopsis*, and other green lineages. *Front. Plant Sci.* 5, 187 (2014).
- Gomez-Porras, J. L. et al. Phylogenetic analysis of K⁺ transporters in bryophytes, lycophytes, and flowering plants indicates a specialization of vascular plants. Front. Plant Sci. 3, 167 (2012).
- 41. Yang, Y. et al. Calcineurin B-like proteins CBL4 and CBL10 mediate two independent salt tolerance pathways in *Arabidopsis*. *Int. J. Mol. Sci.* 20, 2421 (2019)
- 42. Behera, S. et al. Two spatially and temporally distinct Ca²⁺ signals convey *Arabidopsis thaliana* responses to K⁺ deficiency. *New Phytol.* **213**, 739–750 (2017).
- 43. Hedrich, R. & Neher, E. Cytoplasmic calcium regulates voltage-dependent ion channels in plant vacuoles. *Nature* **329**, 833–836 (1987).
- Ward, J. M. & Schroeder, J. I. Calcium-activated K+ channels and calciuminduced calcium release by slow vacuolar ion channels in guard cell vacuoles implicated in the control of stomatal closure. *Plant Cell* 6, 669–683 (1994).
- Pan, Y. et al. Dynamic interactions of plant CNGC subunits and calmodulins drive oscillatory Ca²⁺ channel activities. Dev. Cell 48, 710–725 (2019).
- 46. Tian, W. et al. A calmodulin-gated calcium channel links pathogen patterns to plant immunity. *Nature* **572**, 131–135 (2019).
- Wang, Y. et al. Golgi-localized cation/proton exchangers regulate ionic homeostasis and skotomorphogenesis in *Arabidopsis. Plant Cell Environ.* 42, 673–687 (2019).
- 48. Murashige, T. & S., F. A revised medium for rapid growth and bioassays with tobacco tissue cultures. *Physiol. Plant.* **15**, 473–495 (1962).

Acknowledgements

We thank the Arabidopsis Biological Resource Center for providing *Arabidopsis thaliana* seed stocks. This work was supported by the National Science Foundation (grant nos. MCB-1714795 and ISO-1339239 to S.L.), the Innovative Genomics Institute of the University of California (to S.L.) and the National Natural Science Foundation of China (grant no. 31770266 to E-G.Z.). C.W. is sponsored by the Tang Distinguished Scholarship of the University of California at Berkeley.

Author contributions

R.-J.T. and S.L. conceived and designed the experiments. R.-J.T. performed most of the molecular, genetic and physiological experiments. F.-G.Z. conducted the electrophysiological experiments. Y.Y., C.W. and K.L. assisted in some of the molecular experiments and subcellular localization. T.J.K. and P.G.L. provided some tools and reagents. R.-J.T. and S.L. wrote the manuscript. All the authors discussed the results and commented on the manuscripts.

Competing interests

The authors declare no competing interests.

Additional information

Supplementary information is available for this paper at https://doi.org/10.1038/s41477-020-0621-7.

 $\textbf{Correspondence and requests for materials} \ \text{should be addressed to S.L.}$

Peer review information Nature Plants thanks Ingo Dreyer, Enrico Martinoia and the other, anonymous, reviewer for their contribution to the peer review of this work.

Reprints and permissions information is available at www.nature.com/reprints.

Publisher's note Springer Nature remains neutral with regard to jurisdictional claims in published maps and institutional affiliations.

© The Author(s), under exclusive licence to Springer Nature Limited 2020



Corresponding author(s):	Sheng Luan
Last updated by author(s):	Feb 05, 2020

Reporting Summary

Nature Research wishes to improve the reproducibility of the work that we publish. This form provides structure for consistency and transparency in reporting. For further information on Nature Research policies, see Authors & Referees and the Editorial Policy Checklist.

<u> </u>					
S 1	าล	ŤΙ	ist	Ή.	\sim

For	all statistical analyses, confirm that the following items are present in the figure legend, table legend, main text, or Methods section.
n/a	Confirmed
	extstyle ext
	🔀 A statement on whether measurements were taken from distinct samples or whether the same sample was measured repeatedly
	The statistical test(s) used AND whether they are one- or two-sided Only common tests should be described solely by name; describe more complex techniques in the Methods section.
\boxtimes	A description of all covariates tested
	🔀 A description of any assumptions or corrections, such as tests of normality and adjustment for multiple comparisons
	A full description of the statistical parameters including central tendency (e.g. means) or other basic estimates (e.g. regression coefficient) AND variation (e.g. standard deviation) or associated estimates of uncertainty (e.g. confidence intervals)
	For null hypothesis testing, the test statistic (e.g. <i>F</i> , <i>t</i> , <i>r</i>) with confidence intervals, effect sizes, degrees of freedom and <i>P</i> value noted <i>Give P values as exact values whenever suitable.</i>
\boxtimes	For Bayesian analysis, information on the choice of priors and Markov chain Monte Carlo settings
\boxtimes	For hierarchical and complex designs, identification of the appropriate level for tests and full reporting of outcomes
\boxtimes	Estimates of effect sizes (e.g. Cohen's <i>d</i> , Pearson's <i>r</i>), indicating how they were calculated
	Our web collection on <u>statistics for biologists</u> contains articles on many of the points above.

Software and code

Policy information about availability of computer code

Data collection

WINLAB32 was used to collect ICP-OES data; Opticon Monitor software was used to collect real-time qPCR data; ZEN 2012 was used to collect fluorescence signals from the co-focal microscopy; Clampex 10.3 was used for data acquisition in the patch-clamp experiments.

Data analysis

Microsoft Excel in office 365 and GraphPad Prism 7.0 were used for calculation and statistical analysis of the data; Adobe Photoshop CC2018 was used for image assembly; Clampfit 10.3 was used for data analysis and processing in electrophysiological experiments.

For manuscripts utilizing custom algorithms or software that are central to the research but not yet described in published literature, software must be made available to editors/reviewers. We strongly encourage code deposition in a community repository (e.g. GitHub). See the Nature Research guidelines for submitting code & software for further information.

Data

Policy information about <u>availability of data</u>

All manuscripts must include a <u>data availability statement</u>. This statement should provide the following information, where applicable:

- Accession codes, unique identifiers, or web links for publicly available datasets
- A list of figures that have associated raw data
- A description of any restrictions on data availability

The data that supports the findings of this study are available within the article and its Supplementary Information files or from the corresponding authors upon reasonable request.

Field-spe	ecific reporting
Please select the o	ne below that is the best fit for your research. If you are not sure, read the appropriate sections before making your selection.
Life sciences	Behavioural & social sciences Ecological, evolutionary & environmental sciences
For a reference copy of	the document with all sections, see <u>nature.com/documents/nr-reporting-summary-flat.pdf</u>
Life scier	nces study design
All studies must dis	sclose on these points even when the disclosure is negative.
Sample size	No statistical methods were used to predetermine sample sizes. The exact number of samples in each experiment was specified in the figure legends. In all cases, sample sizes were adequate as the results were reproducible between different experimental groups.
Data exclusions	No data were excluded.
Replication	All attempts to replicate the experiments were successful. Each experiment was repeated for at least three times with similar results obtained. Number of repeats in each experiment was provided in the figure legends.
Randomization	Plants of different genotypes were randomly positioned in the growth chamber or in the greenhouse. Patch-clamp recording on plant cells of different genotypes or plant cells expressing different combinations of exogenous proteins were randomly performed. Randomization was not applied to western blot, ion measurement and qPCR assays.
Blinding	Experiments for reconstitution of the vacuolar potassium efflux current were blinded. One person infiltrated the leaves of Nicotiana benthamiana with multiple combinations of Agrobacteria strains containing different gene constructs, and the other person isolated the vacuoles and did the patch-clamp recording without knowing the sample identity before final data analysis. Blinding was impossible in other experiments because the author who conducted the experiments also performed data acquisition and analysis.

Reporting for specific materials, systems and methods

We require information from authors about some types of materials, experimental systems and methods used in many studies. Here, indicate whether each material, system or method listed is relevant to your study. If you are not sure if a list item applies to your research, read the appropriate section before selecting a response.

Ma	terials & experimental systems	Me	thods
n/a	Involved in the study	n/a	Involved in the study
	Antibodies	\boxtimes	ChIP-seq
\boxtimes	Eukaryotic cell lines	\boxtimes	Flow cytometry
\boxtimes	Palaeontology	\boxtimes	MRI-based neuroimaging
\boxtimes	Animals and other organisms		
\boxtimes	Human research participants		
\boxtimes	Clinical data		

Antibodies

Antibodies used

Rabbit polyclonal Anti-CBL3 and Anti-AtpA: custom-produced by Cocalico Biologicals, Inc. (Stevens, PA); Monoclonal anti-Rabbit secondary antibody: mouse anti-rabbit IgG-HRP provided by Santa Cruz Biotechnology (Cat. No. sc-2357; dilution 1:10000)

Validation

Primary antibodies have been validated by the authors' lab using multiple approaches and experiment results with these two antibodies have been published previously. The secondary antibody has been validated by the manufacture.